Collybistin splice variants differentially interact with gephyrin and Cdc42 to regulate gephyrin clustering at GABAergic synapses

Tyagarajan, S K ; Ghosh, H ; Harvey, K ; Fritschy, J M

Abstract: Collybistin (CB) is a guanine-nucleotide-exchange factor (GEF) selectively activating Cdc42. CB mutations cause X-linked mental retardation due to defective clustering of gephyrin, a postsynaptic protein associated with both glycine and GABA(A) receptors. Using a combination of biochemistry and cell biology we provide novel insights into the roles of the CB2 splice variants, CB2(SH3+) and CB2(SH3-), and their substrate, Cdc42, in regulating gephyrin clustering at GABAergic synapses. Transfection of Myc-tagged CB2(SH3+) and CB2(SH3-) into cultured neurons revealed strong, but distinct, effects promoting postsynaptic gephyrin clustering, denoting mechanistic differences in their function. In addition, overexpression of constitutively active or dominant-negative Cdc42 mutants identified a new function of Cdc42 in regulating the shape and size of postsynaptic gephyrin clusters. Using biochemical assays and native brain tissue, we identify a direct interaction between gephyrin and Cdc42, independent of its activation state. Finally, our data show that CB2(SH3-), but not CB2(SH3+), can form a ternary complex with gephyrin and Cdc42, providing a biochemical substrate for the distinct contribution of these CB isoforms in gephyrin clustering at GABAergic postsynaptic sites. Taken together, our results identify CB and Cdc42 as major regulators of GABAergic postsynaptic densities.

DOI: https://doi.org/10.1242/jcs.086199

Collybistin splice variants differentially interact with gephyrin and Cdc42 to regulate gephyrin clustering at GABAergic synapses

Shiva K. Tyagarajan[1,*], Himanish Ghosh[1], Kirsten Harvey[2] and Jean-Marc Fritschy[1]

[1]Institute of Pharmacology and Toxicology, University of Zurich, 8057 Zurich, Switzerland
[2]Department of Pharmacology, The School of Pharmacy, University of London, London WC1N 1AX, UK
*Author for correspondence (tyagarajan@pharma.uzh.ch)

Accepted 27 April 2011
Journal of Cell Science 124, 2786-2796

doi:10.1242/jcs.086199

Summary

Collybistin (CB) is a guanine-nucleotide-exchange factor (GEF) selectively activating Cdc42. CB mutations cause X-linked mental retardation due to defective clustering of gephyrin, a postsynaptic protein associated with both glycine and $GABA_A$ receptors. Using a combination of biochemistry and cell biology we provide novel insights into the roles of the CB2 splice variants, $CB2_{SH3+}$ and $CB2_{SH3-}$, and their substrate, Cdc42, in regulating gephyrin clustering at GABAergic synapses. Transfection of Myc-tagged $CB2_{SH3+}$ and $CB2_{SH3-}$ into cultured neurons revealed strong, but distinct, effects promoting postsynaptic gephyrin clustering, denoting mechanistic differences in their function. In addition, overexpression of constitutively active or dominant-negative Cdc42 mutants identified a new function of Cdc42 in regulating the shape and size of postsynaptic gephyrin clusters. Using biochemical assays and native brain tissue, we identify a direct interaction between gephyrin and Cdc42, independent of its activation state. Finally, our data show that $CB2_{SH3-}$, but not $CB2_{SH3+}$, can form a ternary complex with gephyrin and Cdc42, providing a biochemical substrate for the distinct contribution of these CB isoforms in gephyrin clustering at GABAergic postsynaptic sites. Taken together, our results identify CB and Cdc42 as major regulators of GABAergic postsynaptic densities.

Key words: Cdc42, Collybistin, GABAaR, Gephyrin, RhoGEF

Introduction

Mutations in *ARHDH9*, encoding collybistin (CB), are a rare cause of X-linked mental retardation (XLMR), with associated features such as seizures, increased anxiety and aggressive behavior (Harvey et al., 2008). These effects are linked to altered trafficking and postsynaptic clustering of gephyrin at inhibitory synapses. Gephyrin is a bi-functional protein contributing to molybdenum cofactor biosynthesis and postsynaptic clustering of glycine receptors (GlyR) and $GABA_A$ receptors ($GABA_AR$) in the central nervous system (CNS) (reviewed in Fritschy et al., 2008). CB is a neuron-specific protein belonging to the Dbl family of guanine-nucleotide-exchange factors (GEFs), which selectively activates the small GTPase Cdc42 (Xiang et al., 2006). *ARHDH9* encodes three CB splice variants (CB1–CB3) with distinct C-termini (Harvey et al., 2004; Kins et al., 2000). All CB isoforms contain a catalytic DH (or RhoGEF) domain and a pleckstrin homology (PH) domain. In addition, alternative splicing of an N-terminal exon encoding a Src-homology 3 (SH3) domain results in CB isoforms containing or lacking the SH3 domain. Curiously, CB3 (also termed hPEM2) (Reid et al., 1999) is the only C-terminal CB splice variant detected in humans to date.

CB was discovered as a gephyrin-interacting protein, facilitating cell surface translocation and clustering with GlyR upon recombinant expression (Kins et al., 2000). So far, the precise function of gephyrin as an anchoring protein has not been elucidated, notably because the mechanisms underlying its clustering at synaptic sites remain elusive. On the basis of structural analysis of its N- and C-terminal domains (designated the G and E domains), gephyrin is considered to form a submembranous scaffold contributing to receptor anchoring at postsynaptic sites (Fritschy et al., 2008; Saiyed et al., 2007). Thus, the CB–gephyrin interaction is believed to regulate gephyrin clustering by modulating intracellular trafficking and scaffolding of gephyrin (Harvey et al., 2004). This hypothesis received further support from the finding that the functional integrity of the PH domain is crucial for CB-mediated gephyrin clustering (Kalscheuer et al., 2009; Reddy-Alla et al., 2010) and from observations that both CB and gephyrin interact with neuroligin-2 (NL2 or NLGN2) (Poulopoulos et al., 2009), a transmembrane protein interacting with presynaptic neurexins selectively localized at GABAergic synapses (Hoon et al., 2009; Varoqueaux et al., 2004).

In addition, CB-mediated activation of Cdc42 is believed to cause remodeling of the actin cytoskeleton stabilizing gephyrin clusters at postsynaptic sites (Xiang et al., 2006). Gephyrin binding to CB has been mapped to the DH domain (Grosskreutz et al., 2001), suggesting a possible regulatory mechanism by gephyrin itself. However, the significance of Cdc42 activation for gephyrin clustering is controversial. Only CB isoforms lacking the SH3 domain induce submembrane gephyrin translocation in non-neuronal cells (Harvey et al., 2004; Kins et al., 2000), although CB isoforms containing the SH3 domain are more common in the CNS. To resolve this paradox, it has been hypothesized that the SH3 domain controls CB enzymatic activity. In particular, NL2 was suggested to regulate $CB2_{SH3+}$ activation by binding to the SH3 domain (Poulopoulos et al., 2009), thereby relieving SH3-mediated autoinhibition of the DH domain (Murayama et al.,

2007). CB binding to the $GABA_AR$ α2 subunit likewise induces cytoplasmic redistribution of gephyrin in non-neuronal cells (Saiepour et al., 2010). However, mutations abolishing DH activity in $CB2_{SH3-}$, as well as genetic deletion of Cdc42 itself, do not impair CB-mediated gephyrin aggregation (Reddy-Alla et al., 2010), calling into question the relevance of CB–Cdc42 interactions for gephyrin postsynaptic clustering.

The generation and analysis of CB-deficient mice unexpectedly revealed that CB is dispensable for proper assembly and function of glycinergic synapses, but is required for proper gephyrin scaffold assembly at specific GABAergic synapses (Papadopoulos et al., 2007). Accordingly, CB-knockout mice show no symptoms of stiffness or increased sensory arousal, which are typical of altered glycinergic transmission (Eulenburg et al., 2005). Rather, these mutant mice exhibit enhanced anxiety, along with impaired long-term potentiation (LTP) in the hippocampal formation. The selective phenotypic alterations displayed by CB knockout mice suggested partial redundancy of CB and Cdc42 functions, and synapse-specific differences in their regulation of gephyrin clustering.

The aim of the present study was to clarify the relevance of CB and Cdc42 activation and their interaction with gephyrin for the regulation of GABAergic synapses. Initial analysis of Myc–$CB2_{SH3+}$ or Myc–$CB2_{SH3-}$ transfected in hippocampal neuronal cultures showed distinct phenotypes with gephyrin clustering. In order to understand the functional basis for the observed phenotypic differences, we used biochemical analysis with purified proteins to identify a new interaction between Cdc42 and gephyrin. In addition, we also identified differences in the biochemical properties between $CB2_{SH3-}$ and $CB2_{SH3+}$ in their ability to form a complex with gephyrin and Cdc42. To understand the functional implications of these biochemical findings, we tested the ability of $CB2_{SH3+}$ and $CB2_{SH3-}$ to cluster gephyrin in the presence of constitutively active (CA) or dominant-negative (DN) Cdc42 mutants. Using laser confocal microscopy, we determine that activation of Cdc42 plays an essential role in the pruning of synaptically localized gephyrin clusters.

Results

$CB2_{SH3+}$ and $CB2_{SH3-}$ influence gephyrin clustering in neurons differentially

CB splice variants lacking the SH3 domain (Fig. 1A) are considered enzymatically active, on the basis of the ability of $CB2_{SH3-}$ to translocate gephyrin to submembranous domains of non-neuronal cells. The CB_{SH3+} isoform, which is predominantly expressed in

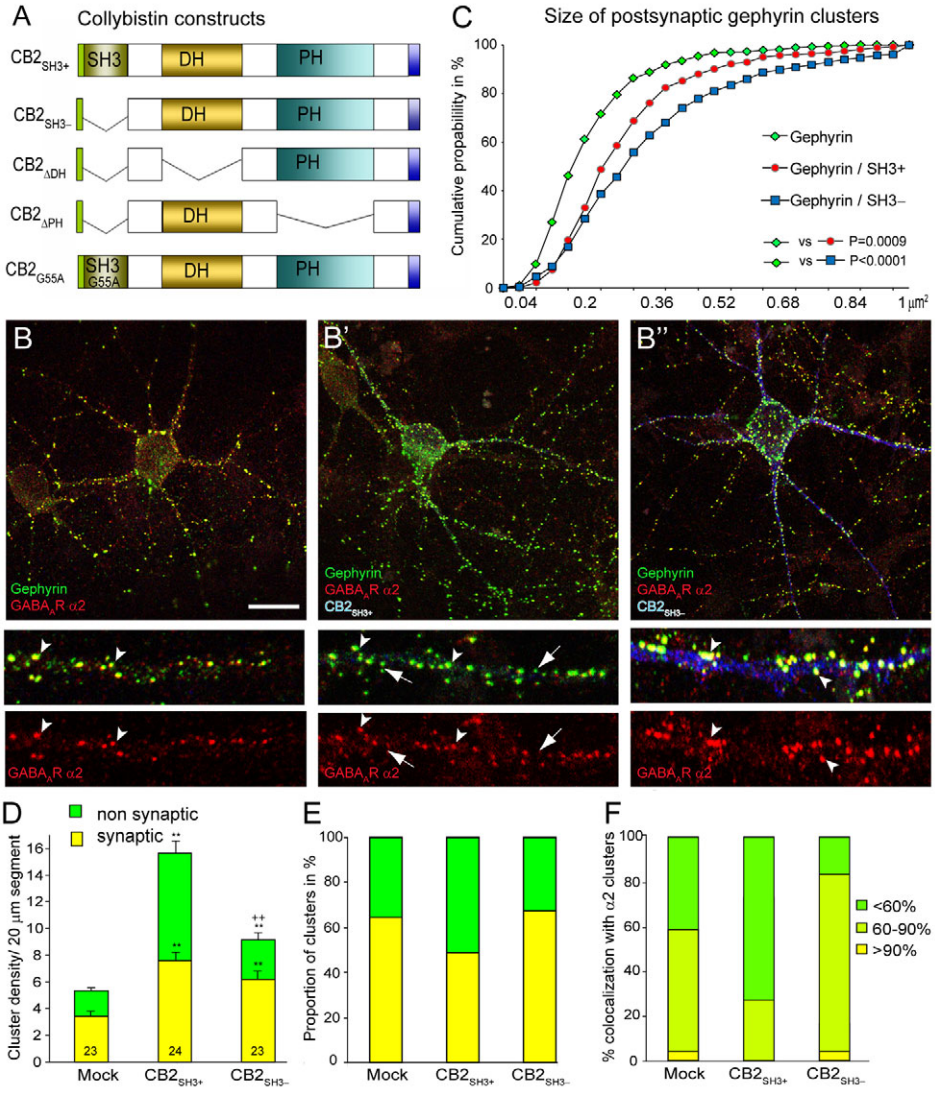

Fig. 1. CB2 splice variants differentially affects gephyrin clustering in neurons. (**A**) Schematic depiction of the CB2 variant cDNA constructs used in this study, omitting the N-terminal Myc tag. (**B–B″**) Transfection of Myc–$CB2_{SH3+}$ and Myc–$CB2_{SH3-}$ differentially affects gephyrin postsynaptic clustering in neurons. Immunofluorescence staining for endogenous gephyrin (green) and $GABA_AR$ α2 subunit (red) in mock-transfected neurons (B) and neurons transfected after 7 DIV with Myc–$CB2_{SH3+}$ (B′) and Myc–$CB2_{SH3-}$ (B″) (blue). Gephyrin clusters per 20 µm dendritic length are shown in the bottom two panels. The arrows point to gephyrin clusters that are not colocalized with the $GABA_AR$ α2 subunit; arrowheads show double-labeled, presumably postsynaptic, gephyrin clusters. (**C**) Cumulative probability distribution of endogenous gephyrin cluster size shows a significant increase in presence of Myc–$CB2_{SH3+}$ or Myc–$CB2_{SH3-}$. (**D**) Quantification of number of synaptic and non-synaptic gephyrin clusters per 20 µm dendritic length shows a significant increase for both Myc–$CB2_{SH3+}$ and Myc–$CB2_{SH3-}$; however, the total number (mean ± s.e.m.) of non-synaptic gephyrin clusters is significantly higher in cells expressing Myc–$CB2_{SH3+}$. $^{**}P<0.01$ relative to mock-transfected cells; $^{++}P<0.01$ relative to $CB2_{SH3-}$ (Bonferroni post-hoc tests). (**E**) The graph represents differences (%) in synaptic compared with non-synaptic gephyrin clusters. (**F**) Changes in the extent of gephyrin cluster colocalization with the $GABA_AR$ α2 subunit, expressed as fraction of dendritic segments containing <60%, 60–90%, and >90% double-labeled clusters in the three populations of neurons analyzed. Myc–$CB2_{SH3-}$ favored the formation of postsynaptic gephyrin clusters. The number of dendrites analyzed in cells from three independent experiments is indicated in each column. Scale bar: 20 µm.

the CNS, has been proposed to stabilize gephyrin at postsynaptic sites by interacting with NL2 and the $GABA_AR$ α2 subunit. However, the functional role of the SH3 domain and the significance of CB activity for gephyrin clustering remain largely obscure. Here, to address these issues, we transiently transfected $CB2_{SH3+}$ and $CB2_{SH3-}$ into cultured neurons, and used immunofluorescence staining to directly visualize and quantify the distribution of gephyrin clusters. We analyzed CB2 splice variants to circumvent potential confounding factors related to the C-terminal sequence differences between CB1 and CB2 (Fig. 1A).

First, we analyzed the effects of Myc-tagged $CB2_{SH3+}$ and $CB2_{SH3-}$ transfection (performed after 7 days in vitro, DIV) on endogenous gephyrin clustering in neurons, as seen 4 days later (7+4 DIV) (Fig. 1A). Postsynaptic gephyrin clusters were identified on the basis of colocalization with the $GABA_AR$ α2 subunit immunoreactivity, detected in living cells with an antibody against its extracellular N-terminal domain (see Materials and Methods). We have shown previously that this approach allows distinguishing between gephyrin clusters located at presumptive postsynaptic sites (double-labeled for the $GABA_AR$ α2 subunit at the cell surface) (supplementary material Fig. S1A) and non-synaptic gephyrin aggregates (Lardi-Studler et al., 2007; Tyagarajan et al., 2010).

In the presence of either $CB2_{SH3+}$ or $CB2_{SH3-}$, the density of endogenous gephyrin clusters was markedly increased compared with that in mock transfected cells (Fig. 1). The increased was particularly striking in the cell body, with transfected cells being outlined by numerous somatic gephyrin clusters. Quantification of gephyrin clusters in dendrites of cells expressing Myc–$CB2_{SH3+}$ revealed a threefold increase compared with that in mock transfected cells (Fig. 1B–B′,D) (ANOVA, $F_{2,68}$=34.154; P<0.0001). Part of this increase was due to the formation of numerous non-synaptic gephyrin clusters, whereas the density of postsynaptic clusters, colabeled for the $GABA_AR$ α2 subunit (and hence postsynaptic; supplementary material Fig. S1A), was doubled (Fig. 1B–B′,D) (ANOVA, $F_{2,68}$=38.934; P<0.0001). As a result, the fraction of synaptic compared with non-synaptic clusters was reduced (Fig. 1F). Overexpression of Myc–$CB2_{SH3-}$ likewise caused an increase in gephyrin cluster density (60%), with the vast majority of the clusters being distinctly double-labeled for the $GABA_AR$ α2 subunit (Fig. 1B″,D,E,F). This increase was specific for gephyrin, as it was not observed for PSD95 (postsynaptic density protein 95, also known as disks large homolog 4, DLG4) (supplementary material Fig. S1B″). Finally, the size of postsynaptic gephyrin clusters was significantly larger in neurons expressing either Myc–$CB2_{SH3+}$ or Myc–$CB2_{SH3-}$ (Fig. 1C). As a control we expressed empty Myc vector instead of Myc–CB2 and did not find any alterations to the gephyrin-clustering phenotype (supplementary material Fig. S1B–B′). Overall, these observations indicate that overexpression of CB2 increases gephyrin clusters, possibly by stabilizing gephyrin and/or facilitating its clustering. These effects are likely to be influenced by the presence of endogenous CB and Cdc42. Nevertheless, the two constructs produce distinct gephyrin-clustering phenotypes, differentiated by the fraction of gephyrin clusters colocalized with the $GABA_AR$ α2 subunit.

The DH and PH domains in CB2 facilitate submembrane gephyrin clustering

In order to understand the functional implications of the PH and DH domains, which are present in all CB splice variants, we co-transfected Myc–$CB2_{\Delta PH}$ or Myc–$CB2_{\Delta DH}$ (Fig. 1A) along with eGFP–gephyrin in cultured neurons, and analyzed for alterations in eGFP–gephyrin postsynaptic clustering (Fig. 2A,B). eGFP–gephyrin was used in these experiments to avoid confounding effects of gephyrin immunofluorescence in double-transfected neurons. Cultures were transfected after 11 DIV and analyzed 7 days later (11+7 DIV), using apposition to synapsin-1-positive

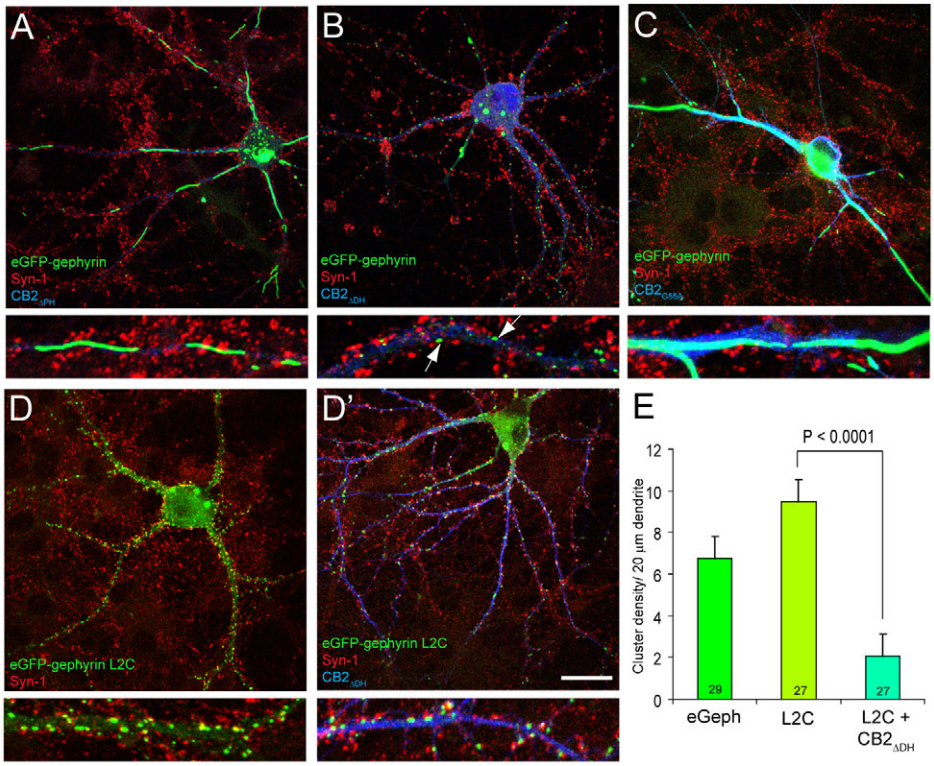

Fig. 2. The PH and DH domains of CB2 are required for proper clustering of eGFP–gephyrin, as demonstrated in double-transfection experiments in cultured hippocampal neurons analyzed at 11+7 DIV. (**A**) Expression of Myc–$CB2_{\Delta PH}$ resulted in the formation of intracellular aggregates and streaks of eGFP–gephyrin. (**B**) Expression of Myc–$CB2_{\Delta DH}$ markedly reduced the density of eGFP–gephyrin clusters, with many being non-synaptic on the basis of apposition to synapsin-1-positive terminals (arrows). (**C**) By contrast, the Myc–$CB2_{G55A}$ mutant construct again abolished eGFP clustering and led to the formation of intracellular streaks, suggesting disruption of the PH domain function, possibly owing to protein misfolding. (**D**–**E**) Absence of the DH domain impairs clustering of the eGFP–gephyrin-L2C construct, known to facilitate formation of gephyrin clusters (Lardi-Studler et al., 2007). Typical examples are illustrated in D–D′. High magnification images of a selected dendritic segment are provided below each overview panel. (E) Quantification of cluster density (mean ± s.e.m.) in cells coexpressing eGFP–gephyrin-L2C and Myc–$CB2_{\Delta DH}$; the number of dendrites analyzed in cells from three independent experiments is given in each column; the P-value was determined by Bonferroni post-hoc test. Scale bar: 20 µm.

terminals to identify postsynaptic eGFP–gephyrin clusters (Tyagarajan et al., 2010). As a control we co-transfected cells with empty Myc vector and eGFP–gephyrin, and this did not affect the gephyrin-clustering pattern (supplementary material Fig. S1B-B″).

Consistent with the presumed importance of the PH domain for membrane targeting of CB and promotion of gephyrin clustering (Reddy-Alla et al., 2010), we observed elongated structures ('streaks') of eGFP–gephyrin in the cell body and neurites of cells expressing Myc–$CB2_{\Delta PH}$ (Fig. 2A), suggesting that gephyrin could not be recruited to the plasma membrane in these cells and therefore aggregated along the cytoskeleton. In cells co-transfected with Myc–$CB2_{\Delta DH}$, eGFP–gephyrin could form postsynaptic clusters (Fig. 2B), albeit with much reduced density, especially compared with cells transfected with Myc-tagged $CB2_{SH3+}$ or $CB2_{SH3-}$ (Fig. 1; see also Fig. 5), suggesting that expression of the C-terminus of CB2 alone could interfere in a dominant-negative fashion with the normal functioning of endogenous CB. This finding further illustrates that gephyrin binding to the DH domain of CB2 facilitates its clustering, as suggested previously by others (Xiang et al., 2006).

We reported previously that a gephyrin chimera (gephyrin-L2C), containing a short bacterial sequence, inserted into the homologous eukaryotic gephyrin sequence is more efficient than wild-type gephyrin at forming postsynaptic clusters in neurons (Lardi-Studler et al., 2007). In order to corroborate the key role of the DH domain on gephyrin cluster formation, we co-transfected neurons with Myc–$CB2_{\Delta DH}$ and eGFP–L2C (Fig. 2D,D′). Quantitative analysis confirmed that eGFP–L2C cluster density on dendrites was strongly reduced in the presence of $CB2_{\Delta DH}$ (Fig. 2E) (ANOVA, $F_{2,80}$=26.366; P<0.001), supporting the hypothesis that gephyrin clustering requires the DH domain in CB2.

A missense mutation, resulting in a G55A replacement in the SH3 domain of $CB3_{SH3+}$, and associated with XLMR, seizures and hyperekplexia, affects gephyrin and $GABA_AR$ clustering in cultured neurons (Harvey et al., 2004). In an attempt to understand the nature of this defect, we speculated that altering the SH3 domain might either directly or indirectly affect the DH domain function (Saiepour et al., 2010). To confirm this hypothesis, we examined neurons co-transfected with Myc–$CB2_{G55A}$ and eGFP–gephyrin (Fig. 2C). A profound alteration of gephyrin clustering was evident, with formation of intracellular streaks similar to those observed with the ΔPH mutant (Fig. 2A). Owing to this striking resemblance with a CB2 mutant unable to target gephyrin to the cell surface, it is likely that the G55A mutation in the SH3 domain affects the PH domain function, possibly owing to protein misfolding.

Gephyrin interacts with Cdc42

Cdc42 is the only CB substrate known so far; it has been postulated to contribute to gephyrin scaffolding by regulating proximal components of the cytoskeleton (Xiang et al., 2006). Furthermore, crystal structure analysis of $CB2_{SH3-}$ bound to Cdc42 has suggested that gephyrin binding at the DH domain of CB2 could compete with Cdc42 binding, thereby blocking the Cdc42 activation by CB2 (Xiang et al., 2006). However, this hypothesis has never been tested experimentally. Hence, we wanted to determine whether Cdc42 plays a role in CB-mediated gephyrin clustering. To achieve this aim, we first tested whether Cdc42 interacts with gephyrin in HEK-293 cells. Co-transfection of Flag–gephyrin and VSVG–Cdc42, followed by immunoprecipitation using antibodies against VSVG and western blotting for Flag–gephyrin, showed that these two proteins formed a complex in this heterologous expression system (Fig. 3A). In order to determine whether this interaction between gephyrin and Cdc42 is direct or occurs through another intermediate molecule, we immobilized bacterially-expressed GST or GST–Cdc42 onto glutathione–Sepharose beads before incubating the beads with bacterially-expressed gephyrin. Prior to adding the purified gephyrin, we incubated the beads with GTPγS or GDP to see whether the Cdc42 activation status influenced its interaction with gephyrin. The two purified recombinant proteins readily interacted with each other in vitro and binding of GTPγS or GDP to GST–Cdc42 did not seem to influence this interaction (Fig. 3A′). Next, we tested whether this interaction also occurs physiologically, for this we used whole brain extracts from adult mice. During the preparation, we separated the cytosolic fraction from the membrane-bound fraction, as we have recently shown that gephyrin is present in both these fractions (Tyagarajan et al., 2010). Immunoprecipitation, using an antibody against gephyrin followed by western blotting for Cdc42, demonstrated that native Cdc42 and gephyrin interact with each other in both the cytosolic and membrane fractions (Fig. 3A″).

Our next aim was to identify the specific gephyrin domain(s) (G and E domains, interconnected by a central linker, the C domain) (see Fritschy et al., 2008) that bind to Cdc42. To this end, we used GST–Cdc42 bound to GTPγS and incubated it with lysates of HEK-293 cells transfected with Flag–gephyrin, or Flag-tagged G, GC or E gephyrin domains (Flag–G, Flag–GC and Flag–E), respectively. Whereas the GST control did not interact with full-length Flag–gephyrin, GST–Cdc42 interacted robustly with Flag–G and Flag–GC (Fig. 3B). Moreover, Flag-E exhibited a weaker interaction for GST–Cdc42, suggesting that there could be two binding sites for Cdc42 on gephyrin (Fig. 3B), with the possibility that the second binding site might overlap with the CB-binding site on gephyrin (amino acids 320–329) (Harvey et al., 2004).

$CB2_{SH3-}$, but not $CB2_{SH3+}$, forms a ternary complex with gephyrin and Cdc42

In order to unravel the mechanistic implications of the Cdc42–gephyrin interaction for regulating CB-mediated gephyrin clustering, we need to better understand how CB interacts with these two partners. We started by looking at the $CB2_{SH3+}$ and $CB2_{SH3-}$ interaction with gephyrin and its individual domains. Although CB binding to gephyrin has been reported previoulsy (Harvey et al., 2004), we wanted to determine whether CB can interact with individual gephyrin domains and also whether gephyrin has more than one binding site for CB. We used purified bacterially-expressed full-length Strep–gephyrin, Strep–G or Strep–E domains and immobilized them on Strep–Tactin beads before adding extracts of HEK-293 cells transfected with either Myc–$CB2_{SH3+}$ or Myc–$CB2_{SH3-}$. Western blotting with antibodies to Myc was used to determine the binding of these CB2 splice variants to gephyrin. Bands positive for Myc–$CB2_{SH3+}$ and Myc–$CB2_{SH3-}$ were readily detectable in lanes containing full-length Strep–gephyrin, but not in lanes containing the Strep–G or Strep–E gephyrin domains (Fig. 4A). These results are consistent with the previous report that the CB-binding site on gephyrin might encompass part of the C domain along with the initial part of E domain, and therefore is detectable only with full-length gephyrin. In addition, these findings confirmed the existence of a single CB-binding site on gephyrin.

Although CB is a RhoGEF selective for Cdc42, the nature of their interaction is still uncharacterized. Hence, we checked whether interaction of $CB2_{SH3+}$ or $CB2_{SH3-}$ with Cdc42 was

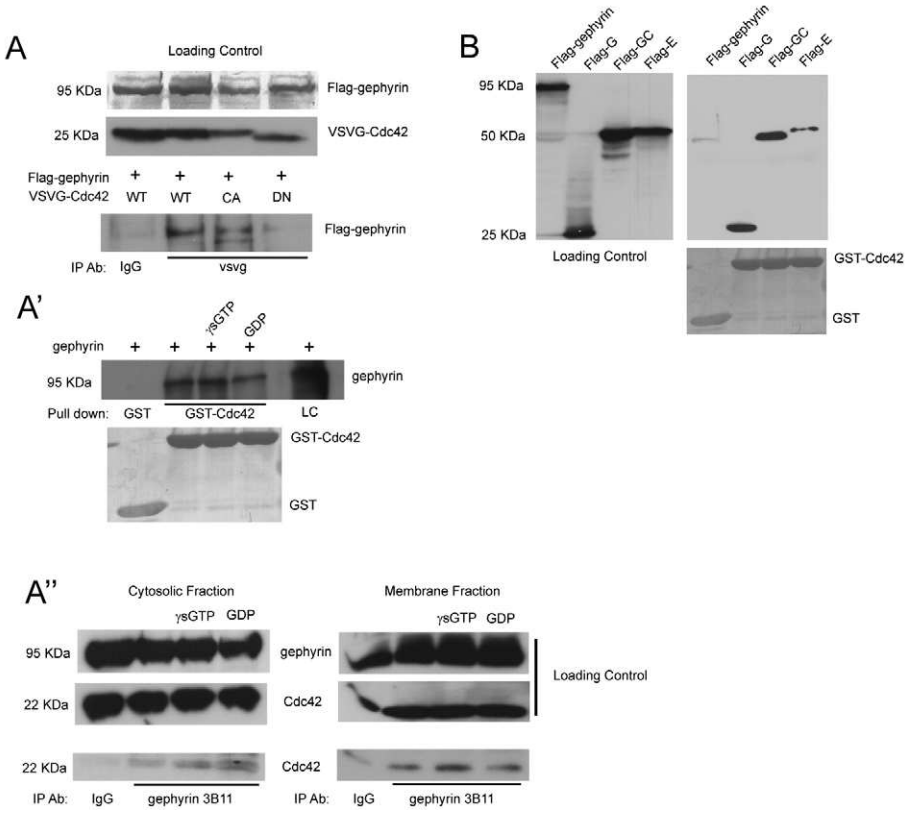

Fig. 3. Cdc42 interacts directly with gephyrin G domain and E domain in vitro and in vivo. (**A**) HEK-293 cells co-transfected with Flag–gephyrin and VSVG-Cdc42. The top panel shows equal expression levels of Flag–gephyrin and VSVG–Cdc42. The bottom panel shows that VSVG–wild-type (WT), constitutively active (CA) and dominant-negative (DN) Cdc42 can interact with Flag–gephyrin using immunoprecipitation (IP) experiments with anti-VSVG antibody, followed by western blotting with mouse anti-Flag antibody. Interaction is weak in the case of DN (lane 4). (**A′**) Bacterial purified full-length gephyrin interacts with bacterially expressed and purified Cdc42 when bound to either GTPγS (γsGTP) or GDP in an in vitro pull-down assay. The gephyrin loading control (LC) shows the amount of gephyrin used in the last lane. The bottom panel shows the levels of GST and GST–Cdc42 in the pull-down assay (Coomassie staining of the blot). (**A″**) The left-hand panel shows Cdc42 interaction with gephyrin in the cytosolic fraction of the brain homogenate. Protein loading controls for gephyrin and Cdc42 are depicted in the top two panels. The bottom panel shows immunoprecipitation for endogenous gephyrin using anti-3B11 antibody, followed by western blot using anti-Cdc42 antibody shows interaction under physiological conditions (lane 2), or in the presence of excess GTPγS or GDP (lanes 3 and 4). The right-hand panel shows Cdc42 interaction with gephyrin in the membrane-associated fraction of mouse brain homogenate. Similar to the cytosolic fraction this interaction is seen in the presence of excess GTPγS or GDP during the immunoprecipitation conditions. (**B**) The left-hand panel shows the expression levels of Flag-gephyrin and its individual domains in HEK-293 cells. The right-hand panel shows the results of a pull-down assay using GST–Cdc42 incubated with HEK-293 lysates overexpressing Flag–G, Flag–GC or Flag–E gephyrin domains. Cdc42 interaction is strong with the G domain, whereas it is weak with the E domain. The bottom panel shows the levels of GST and GST–Cdc42 used in the pull-down assay.

affected by the activation status of Cdc42. We incubated GST–Cdc42 with either GTPγS or GDP shortly before adding lysate from HEK-293 cells transfected with Myc–$CB2_{SH3+}$ or Myc–$CB2_{SH3–}$. Pull-down of GST-Cdc42 followed by western blotting for Myc–CB2 showed that the interaction with Cdc42 was enhanced in the presence of GTPγS, but almost abolished for GDP-bound Cdc42 (Fig. 4A′). A weak interaction could be seen with GST–Cdc42 and Myc–CB2 in the absence of either GTPγS or GDP (Fig. 4A′, lane 2).

Having established that both CB2 isoforms selectively interact with activated Cdc42, we wanted to determine which of them is capable of activating Cdc42 in vivo. By drawing an analogy with other RhoGEFs (Murayama et al., 2007), we speculate that the CB SH3 domain inhibits the DH domain catalytic activity, thereby providing an explanation for why $CB2_{SH3–}$ can mediate translocation of gephyrin to the plasma membrane in non-neuronal cells. In order to test for Cdc42 activation by $CB2_{SH3+}$ and $CB2_{SH3–}$, we used a well-characterized assay system that relies on the interaction between activated Cdc42 and p21-activated kinase 1 (Pak1). Pak1 is a downstream effector of activated Cdc42 and interacts with GTP-bound Cdc42 (Reeder et al., 2001). The minimum sequence required for binding has been mapped and is routinely used to assay for levels of activated Cdc42 inside cells. Hence, we used immobilized GST–Pak1 PBD (Pak1-binding domain) on glutathione beads and assayed for activated Cdc42 in HEK-293 cells expressing either Myc–$CB2_{SH3+}$ or Myc–$CB2_{SH3–}$. Pull-down of GST–Pak1 PBD and western blotting for Cdc42 showed that expression of both CB2 isoforms enhanced the levels of activated Cdc42 in HEK-293 cells (Fig. 4A″). Hence, our data suggest that Myc–$CB2_{SH3+}$ and Myc–$CB2_{SH3–}$ are both capable of activating Cdc42 in vivo. Therefore, the phenotypic differences observed with gephyrin clustering in cells expressing $CB2_{SH3+}$ or $CB2_{SH3–}$ are likely to be unrelated to their enzymatic activity.

So far, our results show that gephyrin interacts with Cdc42 independently of its activation status, whereas $CB2_{SH3+}$ and $CB2_{SH3–}$ interact only with activated (GTP-bound) Cdc42. In

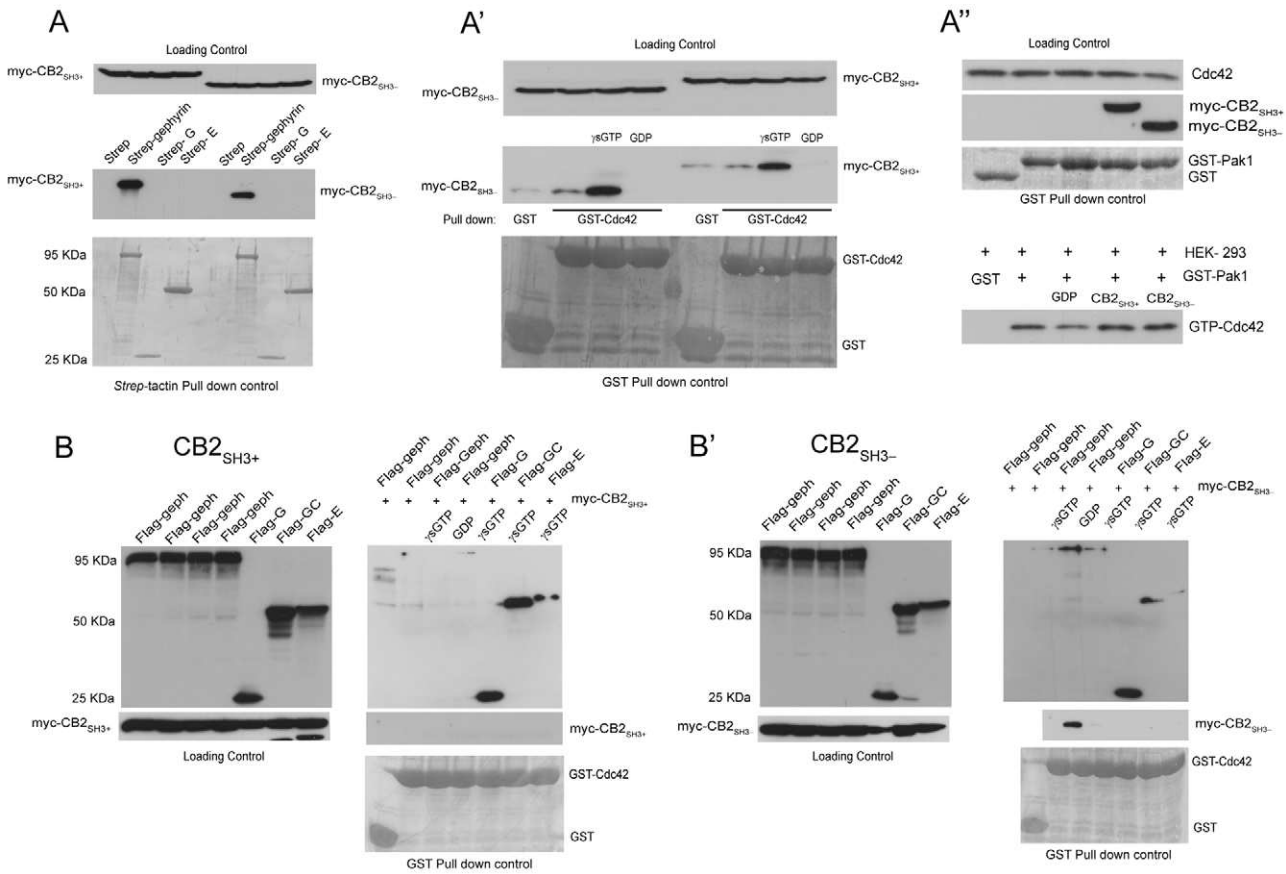

Fig. 4. Cdc42 is differentially regulated by Myc–CB2$_{SH3+}$ and Myc–CB2$_{SH3–}$. (**A**) Myc–CB2$_{SH3+}$ and Myc–CB2$_{SH3–}$ interact with only full-length Strep–gephyrin and not with its individual domains. The top panel shows the expression levels of Myc–CB2$_{SH3+}$ and Myc–CB2$_{SH3–}$ in HEK-293 cells. The middle panel shows Myc–CB2$_{SH3+}$ and Myc–CB2$_{SH3–}$ immunoreactivity after pull-down with immobilized Strep–gephyrin and not with the Strep–G or Strep–E domains. The bottom panel shows Coomassie staining of Strep–gephyrin, Strep–G and Strep–E used in the pull-down assay. (**A′**) Myc–CB2$_{SH3+}$ and Myc–CB2$_{SH3–}$ interact with GST–Cdc42 in the presence of GTPγS (γsGTP) and not GDP. The top panel shows the expression levels of Myc–CB2$_{SH3+}$ and Myc–CB2$_{SH3–}$ in HEK-293 cells used in the pull-down assay. The middle panel shows that immunoreactivity for Myc is highest in the lane where GST–Cdc42 is incubated with GTPγS before the pull-down assay. The bottom panel shows Coomassie staining of GST and GST–Cdc42 used in the pull-down assay. (**A″**) Myc–CB2$_{SH3+}$ and Myc–CB2$_{SH3–}$ can activate Cdc42 equally in HEK-293 cells. The top panel shows the overall levels of Cdc42 in different HEK-293 lysates used in the pull-down assay. The middle panel shows the expression levels of Myc–CB2$_{SH3+}$ and Myc–CB2$_{SH3–}$ in the HEK-293 cells used in the pull-down assay. The lower panel shows Coomassie staining of GST and GST–Pak1 PBD used in the pull-down assay. The bottom panel shows the levels of activated Cdc42 bound by GST–Pak1 PBD in the pull-down assay. The levels of activated Cdc42 are higher in HEK-293 lysates expressing Myc–CB2$_{SH3+}$ or Myc–CB2$_{SH3–}$. (**B**) Myc–CB2$_{SH3+}$ does not form a complex with Flag–gephyrin and GST–Cdc42. The left-hand panel shows the protein expression level for Flag–gephyrin constructs and Myc–CB2$_{SH3+}$ in HEK-293 cell extracts used in the pull-down assay with GST–Cdc42. The right-hand top panel shows a western blot using anti-Flag antibody; weak or no interaction is observed for full-length Flag–gephyrin, whereas we readily detect Flag–G, Flag–GC and Flag–E interaction with GST–Cdc42. The middle panel shows that there is no Myc–CB2$_{SH3+}$ interaction with GST–Cdc42 in the presence of Flag–gephyrin. The bottom panel shows Coomassie staining for GST and GST-Cdc42 in the pull-down assay. (**B′**) Myc–CB2$_{SH3–}$ forms a complex with GTP bound GST–Cdc42 and Flag–gephyrin. The left-hand panel shows Flag–gephyrin and Myc–CB2$_{SH3–}$ protein expression levels in the HEK-293 cell lysates used in the pull-down assays. The top right-hand panel shows a western blot using anti-Flag antibody; Flag–gephyrin, Flag–G and Flag–GC interact with GST–Cdc42 in the presence of Myc–CB2$_{SH3–}$, Flag-E interaction is much reduced or lost. The middle panel shows Myc immunoreactivity for CB2$_{SH3–}$ only in lane 3 where GST–Cdc42 was incubated with GTPγS before the pull-down assay. The bottom panel shows Coomassie staining for GST and GST–Cdc42 used in the pull-down assay.

addition, both CB2 isoforms bind only to full-length gephyrin and can activate Cdc42. These observations raise the possibility that differential complex formation between CB2$_{SH3+}$ and CB2$_{SH3–}$ with gephyrin and Cdc42 underlies their functional differences. In order to test this possibility, we co-transfected HEK-293 cells with Myc–CB2$_{SH3+}$ or Myc–CB2$_{SH3–}$ and either Flag–gephyrin or one of its domains (Flag–G, Flag–GC, Flag–E) and incubated the cell lysates with GST–Cdc42 immobilized onto glutathione beads in the presence of GTPγS. Pull-down of GST–Cdc42 followed by western blotting for Flag demonstrated that binding of full-length Flag–gephyrin to GST–Cdc42 is lost in the presence of CB2$_{SH3+}$ (Fig. 4B); however, the individual gephyrin domains Flag–G, Flag–GC and Flag–E could still interact with GST–Cdc42 (Fig. 4B), as shown above (Fig. 3B). Interestingly, in the presence of CB2$_{SH3–}$, one could still detect interaction of Flag–gephyrin with GST–Cdc42, indicative of a ternary complex formation (Fig. 4B′). Consistent with our observation that CB2 does not bind to isolated gephyrin domains (Fig. 4A), we did not find any Myc–CB2 bands in the lanes containing Flag-G, Flag-GC and Flag-E (Fig. 4B′). Taken together, identification of a

complex between Cdc42, gephyrin and $CB2_{SH3-}$, but not $CB2_{SH3+}$, provides a fresh perspective into the roles of these two CB isoforms in gephyrin cluster regulation. In line with published results, one can hypothesize that the gephyrin translocation to submembranous domains is facilitated by gephyrin–$CB2_{SH3-}$–Cdc42 ternary complex formation, whereas $CB2_{SH3+}$, along with NL2 and $GABA_AR$ (Poulopoulos et al., 2009; Saiepour et al., 2010), might regulate clustering of translocated gephyrin at synaptic sites.

Cdc42 activity regulates the shape and localization of gephyrin clusters

To test our hypothesis, we next investigated how $CB2_{SH3+}$ and $CB2_{SH3-}$ influence gephyrin clustering in the presence of VSVG-tagged Cdc42-CA or -DN mutants, using double and triple transfection in cultured neurons (with eGFP–gephyrin and Myc–$CB2_{SH3+}$ or Myc–$CB2_{SH3-}$). As above (Fig. 2), cells were analyzed at 11+7 DIV, using synapsin-1 staining to identify postsynaptic eGFP–gephyrin clusters. In addition, VSVG–Cdc42 expression was tested by immunofluoresence, but is not shown for simplicity.

In addition, we also tested for the effects of Cdc42-CA and -DN mutants on eGFP–gephyrin postsynaptic clustering in neurons (Fig. 5A–A‴). Overexpression of Cdc42-CA led to formation of numerous, small postsynaptic eGFP–gephyrin clusters (Fig. 5A″), whereas Cdc42-DN led to enlarged clusters (Fig. 5A‴). These observations are in line with a possible role of Cdc42 in regulating gephyrin cluster size at postsynaptic sites.

Overexpression of Myc–$CB2_{SH3+}$ with eGFP–gephyrin replicated the observations made with endogenous gephyrin (Fig. 1B), in particular the increase in density and size of postsynaptic gephyrin clusters (ANOVA, $F_{6,152}$=19.69, P<0.0001), as well as formation of intracellular gephyrin aggregates (Fig. 5B,D,G,H) (ANOVA, $F_{6,152}$=9.688, P<0.0001). Remarkably, coexpression of $CB2_{SH3+}$ with Cdc42-CA or -DN doubled the density of postsynaptic clusters (Fig. 5B″–B‴,G) (ANOVA, $F_{6,152}$=10.151, P<0.0001), suggesting a role for Cdc42 in facilitating gephyrin clustering at synaptic sites, possibly in concert with endogenous CB isoforms. However, Cdc42 activity was the determinant for regulating the size and shape of postsynaptic gephyrin clusters, a significant decrease being observed with VSVG–Cdc42-CA (Fig. 5E), which further confirms the observations made above with Cdc42-CA overexpression (Fig. 5A″).

Neurons co-transfected with eGFP–gephyrin and Myc–$CB2_{SH3-}$ also exhibited a distinctive phenotype, with a large number of postsynaptic gephyrin clusters outlining the cell body and proximal dendrites (Fig. 5C). This observation adds vigor to our hypothesis that $CB2_{SH3-}$ mediates translocation of gephyrin to submembranous sites, possibly by partnering with endogenous Cdc42. A significant increase in postsynaptic eGFP-gephyrin clusters was likewise seen in dendrites (Fig. 5C′,G,H), and the cluster size were considerably enlarged compared with in cells expressing eGFP–gephyrin alone (Fig. 5D).

To determine whether exogenous Cdc42 would further influence the effects of $CB2_{SH3-}$ on gephyrin postsynaptic clustering (Fig. 1B″), we examined neurons triple-transfected with eGFP–gephyrin, Myc–$CB2_{SH3-}$, and VSVG–Cdc42-CA or -DN (Fig. 5C″–C‴). Quantitative analysis of gephyrin clusters showed that Cdc42-CA had no additive effect on the proportion or density of postsynaptic gephyrin clusters on dendrites (Fig. 5G,H), which were not significantly different from those seen in neurons double-transfected with eGFP–gephyrin and Myc–$CB2_{SH3-}$. However, non-synaptic gephyrin aggregates were increased in numbers, suggesting a possible saturation of the machinery targeting gephyrin to postsynaptic sites. Furthermore, both VSVG–Cdc42-CA and -DN led to a significant increase in size of postsynaptic eGFP–gephyrin clusters (Fig. 5F), thereby further accentuating the already strong effect of $CB2_{SH3-}$ (Fig. 5C). However, the shape of these clusters was distinctly different, being regular and round in the presence of Cdc42-CA and irregular and elongated with Cdc42-DN. Taken together, these findings reveal that cooperation between Cdc42 and CB2 isoforms enhances gephyrin postsynaptic clustering and regulates the size and shape of gephyrin postsynaptic clusters, thereby impacting upon GABAergic postsynaptic density.

A major effect of VSVG–Cdc42 overexpression, when combined with Myc–CB2, is to increase the amount of gephyrin clusters in the soma and proximal dendrites (supplementary material Fig. S2A–C). This effect is particularly prominent with $CB2_{SH3-}$ (Fig. 5C″–C‴), in line with its propensity to mediate cell surface translocation of gephyrin. Therefore, Cdc42 might increase the stability of gephyrin, in part independently of its activation status. However, considering the major role of Cdc42 (and other small Rho GTPase family members such as RhoA and Rac1) for cytoskeletal rearrangement, spine formation and synaptic plasticity (Linseman and Loucks, 2008), the differential effects of VSVG–Cdc42-CA and -DN on eGFP–gephyrin clustering might reflect compensatory responses to changes in glutamatergic synapse function. To test this hypothesis, we investigated the effects of neuronal silencing with tetrodotoxin (TTX) on gephyrin clustering in neurons co-expressing Myc–$CB2_{SH3+}$ or Myc–$CB2_{SH3-}$ with the VSVG–Cdc42 mutants. As shown with representative examples (supplementary material Fig. S2D–D′), the eGFP–gephyrin clustering phenotype of triple-transfected neurons is independent of TTX exposure, suggesting that it is due to Cdc42-mediated regulation of CB2 action.

Cdc42-CA rescues gephyrin clustering in the absence of functional PH domain

Mutations in the PH domain preventing CB interaction with membrane phospholipids, such as PtdIns(3,4,5)P_3, affect gephyrin membrane targeting and clustering (Kalscheuer et al., 2009; Reddy-Alla et al., 2010), suggesting a key role in the formation and maintenance of GABAergic synapses. Because the results of our CB2 and Cdc42 co-transfection experiments suggested close functional interactions between these partners, we wondered whether the gephyrin intracellular streaks formed in cells expressing Myc–$CB2_{\Delta PH}$ (Fig. 2A) could be rescued by VSVG–Cdc42-CA. Therefore, we co-transfected neurons with eGFP–gephyrin, Myc–$CB2_{\Delta PH}$, and VSVG–Cdc42-CA and analyzed the gephyrin-clustering phenotype. Introduction of the Cdc42-CA mutant precluded intracellular gephyrin aggregation and led to the formation of postsynaptic clusters (Fig. 6A,A′). Interestingly, co-expression of VSVG–Cdc42-DN could not rescue this phenotype (Fig. 6A″). Thus, this finding suggests that activated Cdc42 can assume the function of targeting gephyrin clusters to submembrane locations or to inhibitory synapses in the absence of a functional CB2 PH domain. Alternatively, activated Cdc42 might enhance the function of endogenous CB sufficiently to rescue gephyrin clustering in cells expressing Myc–$CB2_{\Delta PH}$. In such a case, the availability of free GTP to activate Cdc42 at dendrites might be a limiting factor explaining why this effect is not observed in neurons expressing endogenous Cdc42.

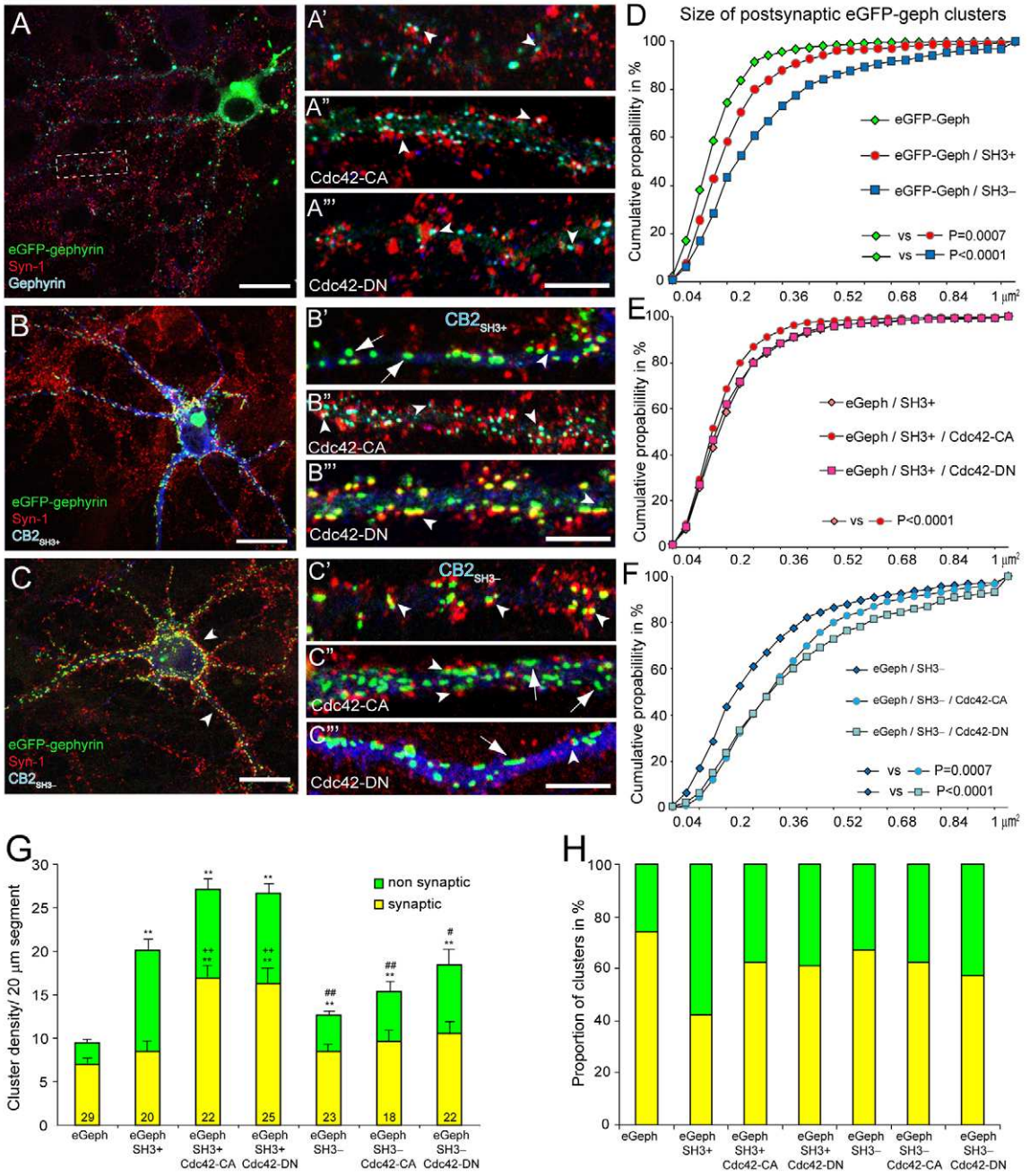

Fig. 5. Cdc42-CA and -DN mutants affect eGFP-gephyrin cluster density and/or size in 11+7 DIV neurons. (**A**,**A′**) Illustration of a neuron transfected with eGFP–gephyrin and stained for the presynaptic marker synapsin-1 (red) and endogenous gephyrin (blue) at 11+7 DIV. The boxed area is enlarged in A′, has arrowheads demonstrating the postsynaptic localization of eGFP–gephyrin clusters. (**A″**,**A‴**) Dendrites from neurons double-transfected with eGFP–gephyrin and VSVG–Cdc42-CA or -DN. Note the regular, round shape of eGFP–gephyrin clusters in the presence of activated Cdc42. (**B**,**B′**) The increase in eGFP–gephyrin cluster density in neurons expressing $CB2_{SH3+}$ is mainly due to the formation of non-synaptic clusters (arrows). (**B″**,**B‴**) Dendrites from neurons triple-transfected with eGFP–gephyrin, VSVG–Cdc42 and Myc–$CB2_{SH3}$; images depict the marked difference in size of postsynaptic eGFP–gephyrin clusters (arrowheads). (**C**,**C′**) In neurons expressing $CB2_{SH3–}$, numerous gephyrin clusters form around the soma and on proximal dendrites (arrowheads). (**C″**,**C‴**) Addition of VSV-Cdc42-CA or -DN causes the appearance of non-synaptic eGFP–gephyrin clusters (arrows) and increases the size of postsynaptic clusters. (**D**) The distribution of postsynaptic eGFP–gephyrin cluster size shows a significant increase in neurons expressing either $CB2_{SH3+}$ or $CB2_{SH3–}$. (**E**) The distribution of postsynaptic eGFP–gephyrin cluster size in neurons expressing Cdc42-CA along with eGFP–gephyrin and $CB2_{SH3+}$ shows a significant size reduction, but has no effect in neurons coexpressing Cdc42-DN. (**F**) The distribution of cluster size in neurons expressing Cdc42-CA or -DN along with $CB2_{SH3–}$ shows a significant increase in size (Kolmogorov–Smirnov tests). (**G**) Absolute changes in the density of synaptic and non-synaptic eGFP–gephyrin clusters (means ± s.e.m.), as normalized per 20 µm dendritic segments. Note the marked increase in non-synaptic cluster density induced by Myc–$CB2_{SH3+}$, whereas Cdc42-CA and -DN mainly increase postsynaptic clusters. In neurons expressing $CB2_{SH3–}$ the amount of non-synaptic cluster density significantly increases with co-expression of Cdc42-CA or -DN. The number of dendrites analyzed in cells from three independent experiments is indicated in each column. $^{**}P<0.01$ relative to mock-transfected cells; $^{++}P<0.01$ relative to $CB2_{SH3+}$; $^{\#\#}P<0.01$ relative to $CB2_{SH3–}$ (Bonferroni post-hoc tests). (**H**) Fractional changes in post-synaptic and extra-synaptic gephyrin clusters in the three populations of neurons analyzed. Scale bars: 20 µm (A–C); 5 µm (A′–A‴, B′–B‴, C′–C‴).

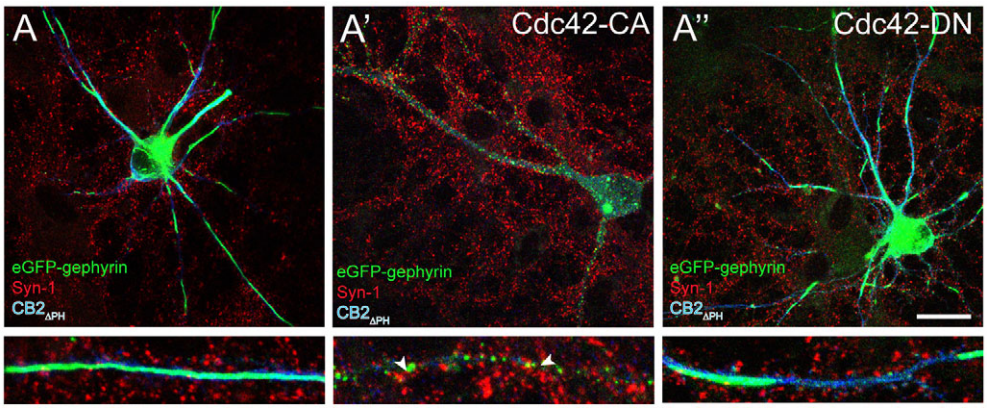

Fig. 6. Co-expression of VSVG–Cdc42-CA, but not VSVG–Cdc42-DN with eGFP–gephyrin (green) and Myc–$CB2_{\Delta PH}$ (blue) rescues postsynaptic gephyrin clustering, as shown by immunofluorescence staining of triple-transfected neurons (11+7 DIV) with synapsin-1 (red). (**A**) Myc–$CB2_{\Delta PH}$ with no Cdc42. (**A′**) Postsynaptic gephyrin clusters are seen in dendrites (arrowheads) and on the soma upon the co-transfection of VSVG–Cdc42-CA. (**A″**) Gephyrin streaks and intrasomatic aggregates are readily evident upon co-transfection of VSVG–Cdc42-DN. Similar results were obtained in three independent experiments. Scale bar: 20 μm.

Discussion

The results of this combined biochemical and cell biological study provide new insights into the roles of the CB2 splice variants, $CB2_{SH3+}$ and $CB2_{SH3-}$, and their substrate, Cdc42, in regulating gephyrin clustering at GABAergic synapses. First, overexpression of $CB2_{SH3+}$ and $CB2_{SH3-}$ in cultured neurons revealed distinct effects on gephyrin clustering, denoting mechanistic differences in their function. Thus, $CB2_{SH3+}$ favored gephyrin aggregation at both synaptic and non-synaptic sites, whereas $CB2_{SH3-}$ selectively increased the density of postsynaptic gephyrin clusters, notably in the soma. Second, overexpression of Cdc42-CA and -DN mutants identified a new function in regulating the shape and size of postsynaptic gephyrin clusters. Finally, the demonstration that $CB2_{SH3-}$, but not $CB2_{SH3+}$, forms a complex together with gephyrin and Cdc42 provides a molecular insight into the underlying functions of these two CB2 isoforms. Taken together, we propose that Cdc42 cooperates with $CB2_{SH3-}$ to translocate gephyrin to the cell surface, whereas interaction of $CB2_{SH3+}$ and its recently identified binding partners NL2 and $GABA_AR$ α2 (Poulopoulos et al., 2009; Saiepour et al., 2010) regulates the formation and maintenance of gephyrin clusters at GABAergic postsynaptic sites through Cdc42 activation independent of the $CB2_{SH3-}$–gephyrin–Cdc42 complex.

Support for this model stems from our data comprising the three independent experiments shown in Fig. 3. First, Cdc42 and gephyrin form a stable interaction that is not dependent on the Cdc42 activation status; in addition, we show that Cdc42 might have more than one interaction site on gephyrin. Second, failure of $CB2_{SH3+}$ to simultaneously bind Cdc42 and gephyrin suggests possible competition between $CB2_{SH3+}$ and Cdc42 for interaction with gephyrin; existence of this competition is underscored by biochemical data showing that Cdc42 interaction with gephyrin G and E domains is unaffected by the presence of $CB2_{SH3+}$, whereas binding to the E domain is lost in the presence of $CB2_{SH3-}$ (Fig. 4B,B′). Third, because there are no apparent differences in the binding of $CB2_{SH3+}$ or $CB2_{SH3-}$ with gephyrin, the availability of Cdc42 appears to be a primary determinant in the regulation of gephyrin clustering. In particular, this competition might explain the formation of non-synaptic aggregates in cells overexpressing $CB2_{SH3+}$. Excess of this CB isoform probably saturates its binding to NL2 and/or $GABA_AR$ at postsynaptic sites, causing $CB2_{SH3+}$–gephyrin complexes to be trapped intracellularly, meaning they cannot be translocated to the cell surface. By contrast, overexpression of $CB2_{SH3-}$ favors formation of ternary complexes, which are readily translocated to the cell membrane, inducing formation of supranumerary gephyrin clusters, probably in collaboration with endogenous $CB2_{SH3+}$ bound to NL2 and/or $GABA_AR$ α2. Although our data and interpretations are based on biochemical evidence and protein overexpression studies, the presence of endogenous CB adds to the existing complexity. Hence, under physiological conditions, competition between gephyrin and Cdc42 for binding to $CB2_{SH3+}$ might be important in regulating delivery of gephyrin at postsynaptic sites, notably its ‘transfer’ from the $CB2_{SH3-}$–Cdc42 transport complex to postsynaptic clusters. Previous work has shown that binding of gephyrin to NL2 is necessary for its clustering at the cell surface (Poulopoulos et al., 2009), suggesting a possible docking of the ternary complex to NL2 before gephyrin incorporation into postsynaptic clusters.

Our study reveals several roles for Cdc42 in the regulation of gephyrin clustering. First, in collaboration with $CB2_{SH3-}$, it greatly favors cell surface translocation of gephyrin, to the point of saturating the endogenous mechanisms regulating postsynaptic gephyrin clustering, as revealed by the formation of numerous gephyrin aggregates in the soma (supplementary material Fig. S2). When $CB2_{SH3-}$ is functionally intact, the activity of Cdc42 is not crucial for this facilitation of gephyrin cell surface translocation. However, the rescue of gephyrin clustering in neurons expressing the functionally-deficient $CB2_{\Delta PH}$ mutant, mediated by Cdc42-CA, but not Cdc42-DN, suggests a functional redundancy between the PH domain of CB2 and activated Cdc42. Because Cdc42 activity plays an important role in localizing cellular proteins at the plasma membrane, it is possible that in the absence of signaling cues from the CB2 PH domain, activated Cdc42 can effectively target gephyrin to submembrane locations. This functional redundancy might explain, at least in part, why Cdc42-knockout mice do not show altered gephyrin clustering at inhibitory synapses (Reddy-Alla et al., 2010) and why gephyrin clustering at GABAergic synapses is affected in a cell-type specific manner in CB-knockout mice (Papadopoulos et al., 2007). Finally, a major new observation is the prominent role of Cdc42 for regulating the

shape and size of postsynaptic gephyrin clusters. This finding is best explained by the interaction of Cdc42 with $CB2_{SH3+}$ at postsynaptic sites, as shown by the co-transfection of the Cdc42-CA and -DN mutants with this CB2 isoform (Fig. 5B″–B‴).

Although failure of $CB2_{SH3+}$ to bind the gephyrin–Cdc42 complex might be explained by a possible steric hindrance from the SH3 domain, it might also reflect the existence of a regulated mechanism. We have shown recently that gephyrin phosphorylation at Ser270 by a GSK3β-dependent mechanism regulates GABAergic synaptogenesis (Tyagarajan et al., 2010). In particular, blockade of GSK3β enhances gephyrin cluster formation by altering Ser270 phosphorylation. Therefore, it is conceivable that dephosphorylation of Ser270 favors binding of $CB2_{SH3+}$ to gephyrin, at the expense of Cdc42, and induces recruitment of NL2 and/or $GABA_AR$ α2 to form a protein complex. This hypothesis would be in line with recent reports that these proteins bind to both $CB2_{SH3}$ and gephyrin (Poulopoulos et al., 2009; Saiepour et al., 2010).

In conclusion, our data reveal that interaction between gephyrin and Cdc42 underlies the clear functional demarcation between $CB2_{SH3+}$ and $CB2_{SH3-}$ in neurons. In addition, direct gephyrin interaction with Cdc42 offers one possible explanation as to why Cdc42 is the only preferred substrate for CB, which is quite unusual for the RhoGEF protein family. A better understanding of differences in the spatial and temporal localization of CB_{SH3+} and CB_{SH3-} isoforms and differences in their upstream activation signals will be necessary to elucidate further the formation and plasticity of GABAergic synapses.

Materials and Methods

Plasmids

The eGFP–gephyrin P1 variant has been described previously (Lardi-Studler et al., 2007). pRK5myc-$CB2_{SH3+}$, pRK5myc-$CB2_{SH3-}$, pRK5myc-$CB2_{G55A}$, pRK5myc-$CB2_{\Delta PH}$, pRK5myc-$CB2_{\Delta DH}$ have been described previously (Harvey et al., 2004). Flag–gephyrin, Flag–G, Flag–GC and Flag–E domains were created after PCR amplifying the respective sequences from eGFP–gephyrin and cloning into pCMV vector using the *Hin*dIII and *Kpn*I sites. pRK-VSVG-Cdc42-CA (QL) and pRK-VSVG-Cdc42-DN (N17) were a kind gift from Kenneth Yamada, NIH, Bethesda. pGEX2T-Cdc42 (Addgene plasmid 12969) has been described previously (Shinjo et al., 1990), pGEX2K-Pak1 PBD (Addgene plasmid 12217) and has been described previously (Sells et al., 1997). One-STrEP-tag gephyrin was created by cloning either the full-length gephyrin P1 variant or its individual domains into pASK-IBA7 vector (IBA, # 2-1406-000) *Eco*RI and *Kpn*I sites.

Cell culture

Primary hippocampal neuron cultures were prepared as described previously (Buerli et al., 2007). Hippocampal cultures were transfected with 1 μg of either eGFP–gephyrin or the specific Myc–CB2 construct according to the protocol described previously (Buerli et al., 2007). Cells were transfected after 11 DIV and processed for immunofluorescence 7 days later (referred to as 11+7 DIV). In co-transfection experiments the total DNA concentration was maintained at 1 μg.

HEK-293-T cells were cultured at 37°C under a 5% CO_2 atmosphere in Dulbecco's modified Eagle's medium (DMEM) supplemented with 10% fetal bovine serum (FBS). They were transfected with 2 μg DNA at 14 hours post plating using polyethylamine (PEI) according to the manufacturer's recommendation. The cells were checked for eGFP protein expression 24 hours post transfection and lysates were prepared for immunoprecipitation and western blot assays.

Immunoprecipitation and western blot analysis

Protein expression in HEK-293 cells was demonstrated using immunoprecipitation assays. The cells were lysed in EBC buffer (50 mM Tris-HCl pH 8.0, 120 mM NaCl and 0.5% NP-40) containing complete mini-protease inhibitor (Roche Diagnostics) and phosphatase inhibitor cocktail 1 and 2 (Sigma–Aldrich). The immunoprecipitation step involved adding specific mouse anti-eGFP or anti-gephyrin antibodies to cell lysates prepared in EBC buffer, incubating the lysate on a rotating wheel at 4°C for 60 minutes and precipitating the antibody–protein complexes using 20 μl Sepharose-A beads (Calbiochem) in EBC buffer. The beads were washed once in EBC-based high-salt buffer (50 mM Tris-HCl pH 8.0, 500 mM NaCl and 1% NP-40) and later twice in EBC buffer. The samples were boiled in 2×SDS sample buffer for 4 minutes at 90°C and the supernatant containing the protein sample was loaded onto the SDS-polyacrylamide gels and run at 140 V at room temperature.

Western blots were performed after transferring the separated proteins onto PVDF membranes. The membranes were blocked using 5% western blocking reagent (Roche Diagnostic) in 1× Tris-buffered saline with Tween 20 (TBST) and later incubated with primary antibody overnight at 4°C. Using a secondary antibody coupled to horseradish peroxidase permitted visualization of protein bands.

The brain homogenates were prepared as described previously (Tyagarajan et al., 2010), and the immunoprecipitation and western blot assays were performed as described above. All animal experiments were performed according to approved guidelines.

GST–Cdc42, GST–Pak1 PBD and Strep–gephyrin were expressed in bacterial strain BL21 pLyss Rosetta to an O.D. of 0.4 and induced with anhydrotetracycline (AHT), as recommended by the vendor (IBA, Germany), for 5 hrs. The bacterial cell pellet was resuspended in EBC buffer containing the protease inhibitor and lysozyme, followed by sonication to disrupt the cells. The lysed cells were centrifuged at 25,000 rpm for 60 minutes and supernatant was aliquoted and frozen at –80°C until further use. Fresh aliquots were used for all experiements, which were thawed and incubated with 20 μl of either glutathione beads (for GST-tagged proteins) and Strep-TACTIN beads (for Strep–gephyrin) for 30 minutes on ice. These were then washed three times in EBC buffer and incubated with either purified bacterially-expressed gephyrin (a gift from Guenter Schwarz, University of Cologne, Cologne, Germany) or lysate of HEK-293 cells overexpressing the desired proteins with epitope tags for 60 minutes in a cold room. The complexes were washed three times in EBC buffer before adding 2× SDS loading buffer and boiling the samples for SDS-PAGE and western blot analysis.

Cdc42 activation assay

GST–Pak1 PBD was overexpressed in bacteria, batch-purified using glutathione beads (20 μl) and washed three times in EBC buffer before proceeding to the next step. The HEK-293 cells were transfected with Myc–$CB2_{SH3+}$ or Myc–$CB2_{SH3-}$ and whole cell lysates were prepared using EBC buffer and added to the GST–Pak1-PBD-bound beads and incubated at 4°C for 60 minutes. The activated Cdc42 was pulled down using GST–Pak1 PBD immobilized onto the beads. The amount of activated Cdc42 pulled down in each of the samples was assayed by western blot for Cdc42.

Antibodies and immunocytochemistry

Mouse anti-gephyrin antibody (mAb7a, 1:3000; or 3B11, 1:10,000; Synaptic Systems, Gottingen, Germany), anti-synapsin-1 antibody (1:500, Molecular Probes, Eugene, OR), guinea pig anti-$GABA_AR$ α2 subunit antibody (Fritschy and Mohler, 1995), mouse anti-Myc (1:10,000, Roche), mouse anti-VSVG antibody (1:5000, Roche) and mouse anti-Cdc42 antibody (1:500, BD Biosciences) were used.

The $GABA_AR$α2 subunit antibody was incubated in living cultures for 90 minutes in culture medium (Brünig et al., 2002). Cells were later rinsed in PBS and fixed for 10 minutes in 4% paraformaldehyde at room temperature. Cells were permeabilized with 0.01% Triton X-100 and detection of intracellular proteins were achieved by incubation for 60 minutes at room temperature with primary antibodies diluted in PBS containing 10% normal serum, followed by incubation with secondary antibodies coupled to Cy3 or Cy5 (1:500, Jackson ImmunoResearch) for 30 minutes at room temperature. Finally, coverslips were mounted with fluorescent mounting medium (Dako Cytomation, Carpinteria, CA).

Image analysis and quantification

Specimens were analyzed using confocal laser-scanning microscopy (LSM 510 Meta, Carl Zeiss, Jena, Germany), using a 100× lens (NA 1.4). Images from each fluorochrome were acquired sequentially using the full dynamic range of the photodetectors, with the pinhole set at 1 Airy unit and a pixel size of 90 nm, and were processed using the Imaris software (Bitplane, Zurich, Switzerland). At least 12 cells from at least three independent batches per condition were used for analysis. Images were acquired as a *z*-stack (2–3 optical sections, 0.5 μm step size). Maximum intensity projections were created from the *z*-stacks and analyzed using image processing and analysis ImageJ software (http://rsb.info.nih.gov/ij/). In each image, one or several dendritic segments were outlined and saved as regions of interest (ROIs). Clusters were defined using the Log 3D plugin, subsequently binary image was used to select specific dendritic regions. The 'analyze particles' tool of ImageJ was used to count the number of clusters (>0.04 μm^2) and to measure their size (area in μm^2). To determine apposition of clusters with presynaptic marker, we increased the size of the cluster area by one pixel all around it edge. To this end a macro was written, to use the log3D-converted image of the dendritic clusters (convert mask to green, use the distance map tool, set threshold to 254–255, convert to mask). The image so obtained was used to quantify apposition between the gephyrin cluster and synapsin-1-positive terminals, with the results incorporated into the ROI manager. The thresholded image of the presynaptic marker staining was then used to show all the analyzed clusters saved in the ROI manager, and the integrated density of the selected clusters was measured. An integrated density value >0 was considered as a gephyrin cluster apposed to the presynaptic marker. In experiments using double-staining between gephyrin and the $GABA_AR$ α2 subunit, postsynaptic clusters were defined based on the colocalization of the two markers in individual clusters. The proportion of single- and double-labeled clusters was determined on the selected ROI.

For statistical analysis of gephyrin cluster size, pair-wise comparisons between constructs were performed by cumulative distribution analysis (Kolmogorov–Smirnov test). For the number of clusters per dendritic segment, mean values were normalized to a length of 20 μm and compared for significance using ANOVA or two-tailed Student's *t*-tests.

We would like to thank Kenneth Yamada (National Institute of Health, USA, Bethesda) for kindly providing the Cdc42 vectors and Guenter Schwarz (University of Cologne, Cologne) for kindly providing bacterial purified full-length gephyrin. We are grateful to Corinne Sidler and Cornelia Schwerdel for technical support, in particular invaluable help with the neuron culture preparation and HEK-293 cell culturing. We thank Abdul Iqbal Mohammed and Marta Raquel Figueiredo for their help with the pull-down experiments and western blots. This study was supported by the Swiss National Science Foundation (grant to J.-M.F.) and the Forschungskredit of the University of Zurich (grant to S.K.T.). K.H. acknowledges support from the UK MRC (G0501258). Deposited in PMC for release after 6 months.

Supplementary material available online at
http://jcs.biologists.org/cgi/content/full/124/16/2786/DC1

References

Brünig, I., Scotti, E., Sidler, C. and Fritschy, J. M. (2002). Intact sorting, targeting, and clustering of γ-aminobutyric acid A receptor subtypes in hippocampal neurons in vitro. *J. Comp. Neurol.* **443**, 43-45.

Buerli, T., Pellegrino, C., Baer, K., Lardi-Studler, B., Chudotvorova, I., Fritschy, J. M., Medina, I. and Fuhrer, C. (2007). Efficient transfection of DNA or shRNA vectors into neurons using magnetofection. *Nat. Protoc.* **2**, 3090-3101.

Eulenburg, V., Armsen, W., Betz, H. and Gomeza, J. (2005). Glycine transporters: essential regulators of neurotransmission. *Trends Biochem. Sci.* **30**, 325-333.

Fritschy, J. M. and Mohler, H. (1995). $GABA_A$-receptor heterogeneity in the adult rat brain: differential regional and cellular distribution of seven major subunits. *J. Comp. Neurol.* **359**, 154-194.

Fritschy, J. M., Harvey, R. J. and Schwarz, G. (2008). Gephyrin, where do we stand, where do we go? *Trends Neurosci.* **31**, 257-264.

Grosskreutz, Y., Hermann, A., Kins, S., Fuhrmann, J. C., Betz, H. and Kneussel, M. (2001). Identification of a gephyrin-binding motif in the GDP/GTP exchange factor collybistin. *Biol. Chem.* **382**, 1455-1462.

Harvey, K., Duguid, I. C., Alldred, M. J., Beatty, S. E., Ward, H., Keep, N. H., Lingenfelter, S. E., Pearce, B. R., Lundgren, J., Owen, M. J. et al. (2004). The GDP-GTP exchange factor collybistin: an essential determinant of neuronal gephyrin clustering. *J. Neurosci.* **24**, 5816-5826.

Harvey, R. J., Topf, M., Harvey, K. and Rees, M. I. (2008). The genetics of hyperekplexia: more than startle! *Trends Genet.* **24**, 439-447.

Hoon, M., Bauer, G., Fritschy, J. M., Moser, T., Falkenburger, B. H. and Varoqueaux, F. (2009). Neuroligin 2 controls the maturation of GABAergic synapses and information processing in the retina. *J. Neurosci.* **29**, 8039-8050.

Kalscheuer, V. M., Musante, L., Fang, C., Hoffmann, K., Fuchs, C., Carta, E., Deas, E., Venkateswarlu, K., Menzel, C., Ullmann, R. et al. (2009). A balanced chromosomal translocation disrupting ARHGEF9 is associated with epilepsy, anxiety, aggression, and mental retardation. *Hum. Mutat.* **30**, 61-68.

Kins, S., Betz, H. and Kirsch, J. (2000). Collybistin, a newly identified brain-specific GEF, induces submembrane clustering of gephyrin. *Nat. Neurosci.* **3**, 22-29.

Lardi-Studler, B., Smolinsky, B., Petitjean, C. M., Koenig, F., Sidler, C., Meier, J. C., Fritschy, J. M. and Schwarz, G. (2007). Vertebrate-specific sequences in the gephyrin E-domain regulate cytosolic aggregation and postsynaptic clustering. *J. Cell Sci.* **120**, 1371-1382.

Linseman, D. A. and Loucks, F. A. (2008). Diverse roles of Rho family GTPases in neuronal development, survival, and death. *Front. Biosci.* **13**, 657-676.

Murayama, K., Shirouzu, M., Kawasaki, Y., Kato-Murayama, M., Hanawa-Suetsugu, K., Sakamoto, A., Katsura, Y., Suenaga, A., Toyama, M., Terada, T. et al. (2007). Crystal structure of the rac activator, Asef, reveals its autoinhibitory mechanism. *J. Biol. Chem.* **282**, 4238-4242.

Papadopoulos, T., Korte, M., Eulenburg, V., Kubota, H., Retiounskaia, M., Harvey, R. J., Harvey, K., O'Sullivan, G. A., Laube, B., Hulsmann, S. et al. (2007). Impaired GABAergic transmission and altered hippocampal synaptic plasticity in collybistin-deficient mice. *EMBO J.* **26**, 3888-3899.

Poulopoulos, A., Aramuni, G., Meyer, G., Soykan, T., Hoon, M., Papadopoulos, T., Zhang, M., Paarmann, I., Fuchs, C., Harvey, K. et al. (2009). Neuroligin 2 drives postsynaptic assembly at perisomatic inhibitory synapses through gephyrin and collybistin. *Neuron* **63**, 628-642.

Reddy-Alla, S., Schmitt, B., Birkenfeld, J., Eulenburg, V., Dutertre, S., Böhringer, C., Götz, M., Betz, H. and Papadopoulos, T. (2010). PH-Domain-driven targeting of collybistin but not Cdc42 activation is required for synaptic gephyrin clustering. *Eur. J. Neurosci.* **31**, 1173-1184.

Reeder, M. K., Serebriiskii, I. G., Golemis, E. A. and Chernoff, J. (2001). Analysis of small GTPase signaling pathways using p21-activated kinase mutants that selectively couple to Cdc42. *J. Biol. Chem.* **276**, 40606-40613.

Reid, T., Bathoorn, A., Ahmadian, M. R. and Collard, J. G. (1999). Identification and characterization of hPEM-2, a guanine nucleotide exchange factor specific for Cdc42. *J. Biol. Chem.* **274**, 33587-33593.

Saiepour, L., Fuchs, C., Patrizi, A., Sassoe-Pognetto, M., Harvey, R. J. and Harvey, K. (2010). Complex role of collybistin and gephyrin in GABAA receptor clustering. *J. Biol. Chem.* **285**, 29623-29631.

Saiyed, T., Paarmann, I., Schmitt, B., Haeger, S., Sola, M., Schmalzing, G., Weissenhorn, W. and Betz, H. (2007). Molecular basis of gephyrin clustering at inhibitory synapses: role of G- and E-domain interactions. *J. Biol. Chem.* **282**, 5625-5632.

Sells, M. A., Knaus, U. G., Bagrodia, S., Ambrose, D. M., Bokoch, G. M. and Chernoff, J. (1997). Human p21-activated kinase (Pak1) regulates actin organization in mammalian cells. *Curr. Biol.* **7**, 202-210.

Shinjo, K., Koland, J. G., Hart, M. J., Narasimhan, V., Johnson, D. I., Evans, T. and Cerione, R. A. (1990). Molecular cloning of the gene for the human placental GTP-binding protein Gp (G25K): identification of this GTP-binding protein as the human homolog of the yeast cell-division-cycle protein CDC42. *Proc. Natl. Acad. Sci. USA* **87**, 9853-9857.

Tyagarajan, S. K., Ghosh, H., Yevenes, G. E., Nikonenko, I., Ebeling, C., Schwerdel, C., Sidler, C., Zeilhofer, H. U., Gerrits, B., Muller, D. et al. (2010). Regulation of GABAergic synapse formation and plasticity by GSK3β-dependent phosphorylation of gephyrin. *Proc. Natl. Acad. Sci. USA* **108**, 379-384.

Varoqueaux, F., Jamain, S. and Brose, N. (2004). Neuroligin 2 is exclusively localized to inhibitory synapses. *Eur. J. Cell Biol.* **83**, 449-456.

Xiang, S., Young Kim, E., Connelly, J. J., Nassar, N., Kirsch, J., Winking, J., Schwarz, G. and Schindelin, H. (2006). The crystal structure of Cdc42 in complex with collybistin II, a gephyrin-interacting guanine nucleotide exchange factor. *J. Mol. Biol.* **359**, 35-46.